THE JOURNAL OF PHYSICAL CHEMISTRY Letters

Letter

pubs.acs.org/JPCL

Effects of Exciton Polarity in Charge-Transfer Polymer/PCBM Bulk Heterojunction Films

Brian S. Rolczynski,[†,‡,§] Jodi M. Szarko,[†,‡,§,⊗] Hae Jung Son,[‡,∥,⊥] Luping Yu,[*,‡,∥] and Lin X. Chen[*,†,‡,§]

[†]Department of Chemistry and [‡]ANSER Center, Northwestern University, 2145 Sheridan Road, Evanston, Illinois 60208, United States

[§]Chemical Sciences and Engineering Division, Argonne National Laboratory, 9700 South Cass Avenue, Argonne, Illinois 60439, United States

[∥]Department of Chemistry and The James Franck Institute, The University of Chicago, 929 East 57th Street, Chicago, Illinois 60637, United States

Supporting Information

ABSTRACT: Charge-transfer copolymers with local electron density gradients, systematically modified by quantity and position of fluorination, result in widely variable (2−8%) power conversion efficiencies (PCEs). Ultrafast, near-infrared, transient absorption spectroscopy on the corresponding films reveals the influence of exciton polarity on ultrafast populations and decay dynamics for the charge-separated and charge-transfer states as well as their strong correlation to device PCEs. By using an excitation energy-dependent, dynamic red shift in the transient absorption signal for the polymer cation, the exciton polarity induced by push−pull interactions within each polymer fragment is shown to enhance charge dissociation on time scales of tens to hundreds of picoseconds after excitation. These results suggest the important role played by the local electronic structure not only for exciton dissociation but also for device performance.

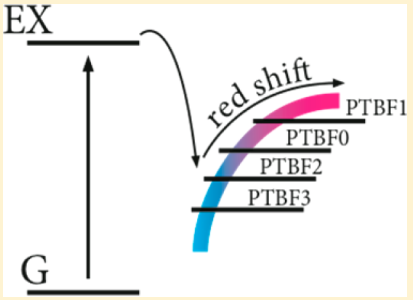

SECTION: Energy Conversion and Storage; Energy and Charge Transport

Organic photovoltaic (OPV) devices have great potential for renewable, clean, cost-effective energy production.[1−3] However, one of the main challenges is their relatively low power conversion efficiency (PCE) with respect to their inorganic counterparts.[4] In the past several years, the PCEs of OPV devices have almost doubled from 5% to nearly 10% in single junction devices.[5] One of the key factors responsible for such significant improvements in PCEs is the incorporation of charge-transfer polymers (CTPs). In contrast with homopolymers such as poly(3-hexylthoiphene) (**P3HT**), which contain identical blocks along the polymer backbone, CTPs are composed of distinct building blocks with different electron affinities in each repeating unit of the polymer. As a result, they form $(\mathbf{d}\text{-}\mathbf{a})_n$ sequences, where n is the number of the repeating units of the polymer and **d** and **a** are adjacent blocks with some degree of donor−acceptor character (Figure 1c). Meanwhile, complete charge separation is observed in bulk heterojunction (BHJ) films where the polymer is the electron donor (**D**) and fullerene derivatives are the electron acceptor (**A**) (Figure 1c).[6] Although the initial design ideas for these CTPs were focused on adding quinoidal character to the polymer, which induces a charge-transfer (CT) band to enhance the light harvesting in the red and near-IR regions of the solar spectrum, the CT character in CTPs has brought profound effects in the exciton (EX) dissociation, charge separation, and charge migration steps in the bulk heterojuction (BHJ) devices with an active layer composed of these **D**−**A** pairs (Figure 1b).[7−9] One family of these CTPs, the poly(thienothiophene-benzodithiophene) (**PTB**) series, has established new PCE records previously set by **P3HT**. Understanding why these CTPs could improve device PCEs at the fundamental steps of OPV function is important for establishing design guidance to modulate their properties via chemical modification because both their molecular properties and corresponding device PCEs are highly sensitive to small differences in local molecular structure.[10−12]

A clear correlation has previously been observed between the charge-carrier population and the driving force for exciton dissociation in BHJ OPV films containing homopolymers or CTPs as **D** and fullerene derivatives such as phenyl-C_{61}-butyric acid methyl ester (**PCBM**) as **A**.[9,13] An anomalous deviation was found in certain CTPs by Durrant and coworkers, which has higher yields of charge-carrier population despite a much smaller apparent LUMO−LUMO energy offset, which is an estimate of the driving force for electron transfer from the exciton of the polymer to **PCBM**.[9,13] The driving force can also be approximated by comparing the ionization potential and electron affinity of the donor and acceptor, respectively. This unexpected result prompts reconsideration of the driving force

Received: March 26, 2014
Accepted: May 13, 2014

   dx.doi.org/10.1021/jz5005957 | J. Phys. Chem. Lett. 2014, 5, 1856−1863

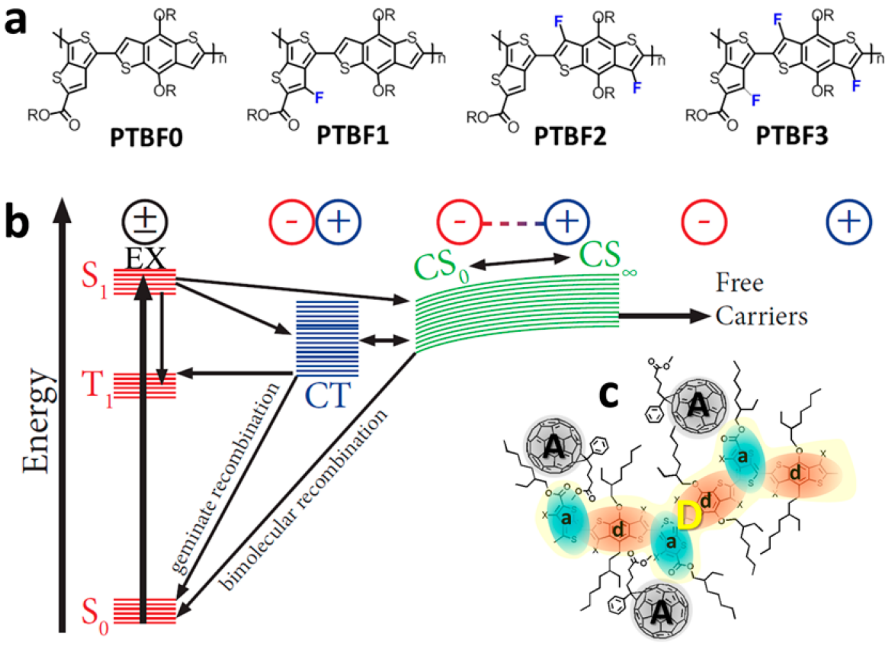

Figure 1. (a) **PTBF** polymers. (b) Possible intermediate states and their energy levels in BHJ films. (See the text.) (c) Illustration of **-d-a-** motifs and donor (D) polymer and fullerene acceptor (A).

effect in these CTPs and the dependence of the driving force relationship to the exciton and charge-carrier dynamics in CTP BHJ films. In our recent studies on the **PTBF** CTP series (Figure 1a), in which zero to three electron-withdrawing fluorine atoms are connected to different positions of the CTP backbone, we reported the effect of the local CT character of the **-d-a-** motif on the initial cation populations, even in solution without **A**.[7,8,14] Key findings from this solution study indicated the following: (1) significant polymer cation populations, corresponding to charge-separated (CS) populations, were generated via intramolecular exciton dissociation within 100 fs after excitation; (2) this initial cation (or positive polaron as referred by some) population is closely correlated to the local structure that determines the exciton polarity by electron-withdrawing fluorine atoms at different peripheral positions of the polymer backbone; (3) the local exciton polarity, or the displacement of the positive and negative charge densities in the exciton due to the CT character in the CTPs, defrays a part of the driving force required for further exciton dissociation; and (4) the polymers with higher initial CS populations (**PTBF0** and **PTBF1**) have higher PCE in the corresponding devices, while the polymers with higher initial CT populations (**PTBF2** and **PTBF3**) result in lower PCE in the devices.[7,15,16]

What needs to be studied further is how the local CT character in CTPs affects exciton dissociation at **D-A** boundaries in BHJ films used in OPV devices and the resulting CS populations. Because EX dissociation and CS state generation were observed in <100 fs after excitation in these CTPs, the promptly generated EX population may not have relaxed yet, and the exciton size is still unclear and debatable in these CTPs.[17] Hence, it is difficult to define quantitatively the exciton polarity based on polymer structures or the HOMO−LUMO electron density distribution. Instead we use a calculated figure of merit, the local dipole moment change between the ground and first excited states in each **d-a** motif of the **PTBF** polymers, to characterize the local exciton polarity defined by $\Delta\mu_{eg} = \mu_e - \mu_g$ (where μ_e is the excited-state dipole and μ_g is the ground-state dipole of the polymer).[6,7,15,16] Although this value could be diverse due to the different isomers produced via the rotation along certain C−C bonds along the polymer chain,[18] its averaged value should reflect the ensemble in a series of CTPs with identical backbones such as the **PTBF** polymers (Figure 1). This figure of merit was justified in our previous study on the **PTBF** polymers in solution, which showed that a higher $\Delta\mu_{eg}$ gives a higher initial population ratio of the polymer cation, representing the CS state, to the bound pairs representing the CT state.[7] Here we report our studies of these systematically altered **PTBF** polymers in BHJ films, focusing on the role of the local exciton polarity on the exciton dissociation dynamics at the **D-A** interface between CTPs and **PCBM** using near-infrared (NIR) transient absorption (TA) spectroscopy.[7] In particular, we focus on the importance of local structure in **-d-a-** motifs of these **PTBF** CTPs on exciton dissociation dynamics over a time scale of approximately 100 fs to 100 ps in BHJ films as well as the corresponding device properties. The results on these time scales elucidate the characteristics of the following mechanisms in BHJ films: (1) the degree of electron transfer in the CTP BHJ films, (2) the dissociation of the cationic species from its anionic counterpart, (3) the dependence of the local electronic structure on the Coulombic interaction between charges in the D and A species, and (4) the excitation energy dependence on the dissociation time of the exciton. Such studies will provide guidance in designing high-efficiency BHJ materials for high-performance OPV devices.

The general exciton dynamics and photophysical pathways are illustrated in Figure 1b. The most important three transient species, EX (exciton), CT (charge transfer), and CS (cation), all have absorption in the NIR region.[7] The NIR TA spectra for each of the **PTBF** polymers in BHJ films exhibit a broad absorption signal across the 900−1400 nm window at early delay times (i.e., <1 ps) (Figure 2a), reflecting the energy distribution of the transient species' highly disordered

dx.doi.org/10.1021/jz5005957 | J. Phys. Chem. Lett. 2014, 5, 1856−1863

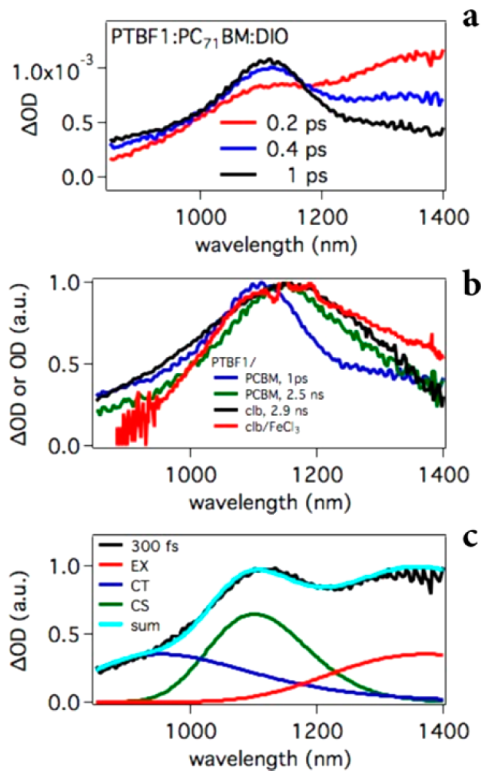

Figure 2. (a) Transient spectra of the **PTBF1** BHJ film. (b) **PTBF1** spectra of the polymer cation, obtained by oxidation with **$FeCl_3$** (red), TA at 2.9 ns delay in chlorobenzene (clb) **PTBF1** solution (black), and TA at 1 ps (blue) and 2.5 ns (green) delay in **PTBF1/$PC_{71}BM$/DIO** BHJ film. (c) TA signal of **PTBF1** at 300 fs delay is plotted as well as the fitted peaks for EX, CT, and CS and the sum of these three peaks. The fit peaks appear asymmetric in wavelength because they were modeled as Gaussian in energy space.

structures in the BHJ films. Careful examination of these BHJ film TA spectra (Figure 2a) at different delay times confirms the following key observations: (1) the TA feature at the 1300−1400 nm region, which is assigned to the EX state, decays faster than signals elsewhere in the TA spectral window; (2) the TA feature centered at 1150 nm rises as the TA signal at 1300−1400 nm decays; and (3) the signal peaked at ∼1150 nm retains considerable intensity well beyond a few nanoseconds and decays more slowly than the TA features elsewhere in the TA spectral window. Because the TA feature in the 1300−1400 nm region appears at the earliest delay time and decays with the concurrent rise of the TA feature centered at ∼1150 nm in the BHJ film, the 1150 nm region is assigned to the polymer cation absorption of the CS state, and this assignment is confirmed by the absorption spectra of oxidized polymers in solution titrated with $FeCl_3$ as an oxidant (Figure 2b).[7] For the assignment of the 900−1100 nm feature, we have considered different possibilities, such as a triplet state, **$PC_{71}BM$** anion, and the CT state. In the CT state, the hole and electron after exciton dissociation are only separated at a short distance and are strongly interacting due to Coulombic attraction. The triplet states can be ruled out because the ultrafast formation (within the IRF) of this feature is too short for intersystem crossing in conjugated polymers,[8,19,20] and the **$PC_{71}BM$** anion can be ruled out because the decay kinetics differ from those of the CTP cation on geminate recombination time scales both in solution[7] and BHJ films. (See later.) Therefore, the most likely assignment for the 900−1100 nm feature is the CT state, as in the corresponding solution samples.[7]

Using a global fitting method,[7] the TA spectra in the NIR region of BHJ films were fit to three Gaussian components B_x, where x corresponds to the three transient species: EX, CT, or CS. The number of simultaneous fitting parameters was minimized by fixing several of the parameters at independently deduced values. (See the Supporting Information.) The kinetics of these B_x components were obtained by fitting each component in the transient spectrum to yield kinetic traces

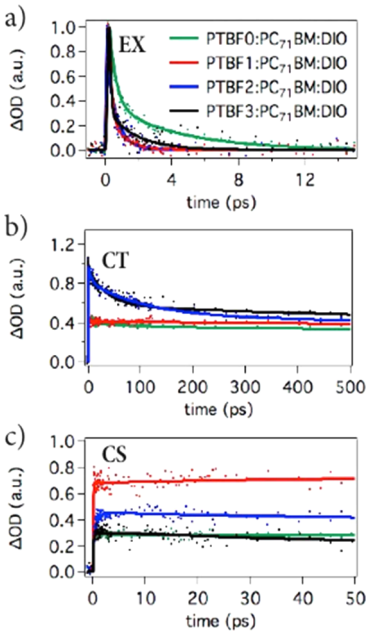

Figure 3. BHJ film transient absorption dynamics of the **PTBF** series are shown, normalized by the EX signal intensity.

(Figure 3). These traces subsequently were fit to n exponential decays and a Gaussian instrument response function (eq 1).

$$\Delta \mathrm{OD}_x(\omega, t) = \sum_n A_n^x(\omega) \exp\left(-\frac{t}{\tau_n^x}\right) * \exp\left[-\frac{1}{2}\left(\frac{t - t_0}{\sigma}\right)^2\right] \quad (1)$$

In this equation, x denotes EX, CT, or CS; n is the index of the exponential components; τ_n^x are time constants; t is the time delay between the pump and probe pulses; t_0 is time zero; σ is the temporal width of a Gaussian instrument response function; and $A_n^x(\omega)$ is the pre-exponential weight of the nth exponential component of transient species x at the probe energy proportional to ω.

On the basis of the global fitting previously mentioned, the kinetics of the EX, CT, and CS populations in BHJ films are obtained (Figure 3, and Table S1 in the Supporting Information). The majority (A_1^{EX} = 70−87%) of the initial EX state population in the BHJ films decays with a time constant of 100−400 fs after photoexcitation, and the entire EX population decays within 10 ps for all films. A concurrent rise is observed in the CS signals of **PTBF2** and **PTBF3**. The ∼100 fs, dominating EX decay kinetics appear only in the presence of **PCBM**, suggesting their association with intermolecular CT from the polymer to **PCBM** as a result of exciton dissociation. This result is consistent with other BHJ systems with sufficient

dx.doi.org/10.1021/jz5005957 | J. Phys. Chem. Lett. 2014, 5, 1856−1863

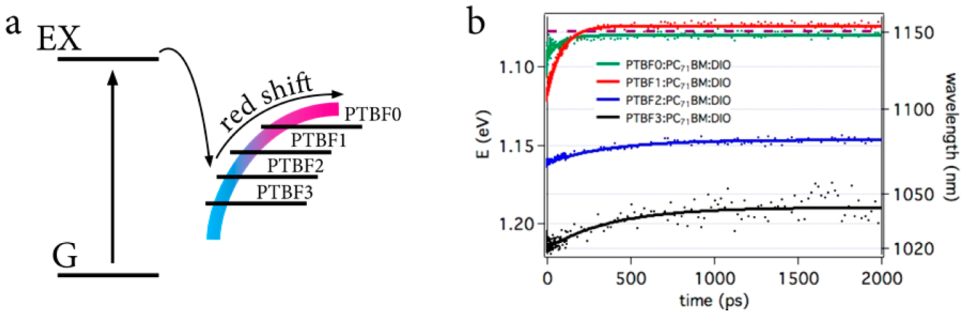

Figure 4. (a) Schematic of the dynamics revealed by the red shift dynamics revealed in part b. The color scheme indicates the wavelength of the CS feature as it detraps at the donor−acceptor interface. (b) CS (cation) peak position in energy (left axis) and wavelength (right axis) of **PTBF** polymers versus pump−probe delay time. The line shape of these curves represents a red shift of the transient CS signal, while the final CS peak energy indicates the average energy of the CS population after the fast dissociation process has occurred. The purple dotted line at 1.078 eV indicates the baseline obtained from the peak positions of each polymer's CS feature in transient solution studies.

intercalation.[16−18,36−43] Similar to the solution case, the CT feature in 900−1100 nm region in the BHJ films is consistently more pronounced for **PTBF2** and **PTBF3** at earlier times than in corresponding **PTBF0** and **PTBF1** TA spectra.

While the CS peak positions for all polymers in solution remain at ∼1150 nm (1.078 eV) up to ∼3 ns after excitation,[7] these features initially appear significantly blue-shifted from 1150 nm in the corresponding BHJ films and subsequently undergo a continuous red shift to different steady-state positions. Therefore, the position of the CS peak was allowed to vary in the fitting procedure. The CS peak positions for **PTBF0** and **PTBF1** in BHJ films shifted to ∼1150 nm to match those in solution within 100 ps, whereas those for **PTBF2** and **PTBF3** remained significantly blue-shifted of their corresponding 1150 nm solution peaks with four to five times slower peak shift time constants. The initially blue-shifted cation TA feature suggests a larger energy gap, which is reduced over time, between the cation and the upper states that are populated by probe photon absorption. Because the final peak positions are identical for all polymers in solution but differ in films of **PTBF2** and **PTBF3**, (a) the early time stabilizations of the CS state energies for **PTBF2** and **PTBF3** are lower than those for **PTBF0** and **PTBF1** in the BHJ films and (b) considering the sustained blue shift at ∼3 ns relative to their solution positions, the **PTBF2** and **PTBF3** cations remain partially stabilized in BHJ films, while the other polymers' cations do not. This difference among the **PTBF** polymers can be ascribed to counterion stabilization, where the oppositely charged, proximal hole and electron from a dissociated exciton stabilize each other relative to when they are fully separated.[21−26] The electron from the dissociated exciton, localized on **$PC_{71}BM$** as an anion, can take that role to stabilize the polymer cation when these species are proximal. This is possible because, in a 3-D space, the entropy of two initially colocalized charge carriers diffusing apart face an energy barrier on the order of k_BT at room temperature.[27] In addition, the **PTBF** polymers form a mixed phase with **$PC_{71}BM$**,[6] resulting in only ∼20% crystalline regions within the **PTBF1** BHJ film, for instance.[28] The initial cation peak energies in these four **PTBF** polymers follow the same order as the energies of their HOMOs, **PTBF0** > **PTBF1** > **PTBF2** > **PTBF3**, suggesting that the cations are stabilized most in **PTBF3** and least in **PTBF0**. This trend, which only occurs when the polymer is in the presence of **PCBM**, can be understood as an effect of the electron density depletion in the backbone of the polymers. The fluorine atoms draw electron density toward the periphery and lower the net electron density on the backbone, which is equivalent to increasing the positive charge from the perspective of a nearby **PCBM** anion and therefore enhances the electrostatic interaction between the **D-A** pair, localizing the CS state. **PTBF3** has the lowest electron density on the backbone, so it has the lowest energy for the cation or CS state. The stronger Coulombic attraction between the anionic **PCBM** and cationic **PTBF** near the **PTBF-PCBM** interface adequately explains the initial blue shift of the CS (cation) peak in the **PTBF** film spectra compared with those in solution, where the intramolecular charge separation is screened by the surrounding solvent molecules.

When comparing the cation peak energies for all four **PTBF** polymers in solution and in BHJ films, we observed the dependence of the cation dynamics in the two media in terms of (1) the initial cation peak energy, (2) the peak position shift; (3) the local structure-dependent kinetics for the peak shift, and (4) the excitation energy dependence of the cation dynamics. As previously discussed, the cation peak positions for all four polymers in solution are unchanged from 100 fs to a few nanoseconds after excitation,[7] but they shift to longer wavelengths continuously in the corresponding BHJ films on the time scale of <100 ps to several hundred picoseconds. About 80 ps after excitation, the BHJ cation peak positions made from **PTBF0** and **PTBF1** red shift to approximately the same energy (1.08 eV) as those in solution. In contrast, the corresponding cation peaks in the BHJ films made from **PTBF2** and **PTBF3** remain at higher energies ∼3 ns after excitation (Figure 4). The magnitudes of the red-shifted energies $E_S = E_{CS}(3\text{ ns}) - E_{CS}(0)$ for all samples are within a factor of 2 of k_BT at room temperature (26 meV) (Figure 4a). Additionally, E_S is dependent on excitation energy. The red shifts in Figure 4 result from 600 nm light excitation. When the **PTBF1** BHJ films are excited by 695 nm light at the red edge of the ground-state absorption spectrum, the cation peak begins at a similar energy but exhibits a drastically slower red shift and does not reach 1150 nm within the 3 ns measurement window.[6] The red shift of the CS (cation) peak occurs when the geminate hole−electron pair further separates,[29] weakening Coulombic attraction. This dissociation process can be assisted by local thermal energy derived from excess excitation energy, explaining the excitation-wavelength-dependent red shifts within a factor of 2 of k_BT.[6] Within the time window of the TA experiments (∼3 ns), the cation peak position in solution sets an approximate limit of the red shift, resulting from the well-screened cationic species in the absence of anionic **PCBM**.

dx.doi.org/10.1021/jz5005957 | J. Phys. Chem. Lett. 2014, 5, 1856−1863

As shown in Figure 4, the extent and lifetime of the red shifts depend on the local structure of the repeating units of the polymers. The electron density push−pull character modulated by electron-withdrawing fluorine atoms can also influence hole−electron dissociation behavior at BHJ interfaces. The kinetics of the cation peak red shifts can be modeled by a single exponential function using the initial ($E_{CS}(0)$) and final ($E_{CS}(3$ ns)) peak energies of the cation: $E_{CS}(t) = [E_{CS}(0) - E_{CS}(3$ ns)]e^{-t/τ_S}, where τ_S is the time constant for the red shift. τ_S is smaller for **PTBF0** and **PTBF1** than for **PTBF2** and **PTBF3**. The τ_S values for both **PTBF0** and **PTBF1** are ∼77 ps, but those for both **PTBF2** and **PTBF3** are ∼380 ps. Likewise, $E_{CS}(3$ ns) for **PTBF0**, **PTBF1**, **PTBF2**, and **PTBF3** are 1.080, 1.074, 1.147, and 1.19 eV, respectively. The larger the energy difference between $E_{CS}(0)$ and the solution intramolecular CS state,[7] the stronger the Coulombic attraction (or "trap," not to be confused with the free carrier trap sites that are important at longer time scales[9]) for the geminate charge pair. Therefore, the CS electron−hole pairs in **PTBF2** and **PTBF3** are Coulombically trapped more deeply and dissociate more slowly, while they are not trapped as deeply and dissociate more quickly in **PTBF0** and **PTBF1**. Thus, E_S describes the cation energy change, as the cation separates from the anion to escape from the Coulombically stabilized CTP-**PCBM** interface. The magnitude of E_S is near k_BT, suggesting that the population with Coulombic attraction equal to or less than the ambient energy can be dissociated via the thermal energy generated due the vibrational relaxation that converts the excess excitation energy to heat.

The Role of Intrinsic Charge Transfer Character in Exciton Dissociation Dynamics. Intramolecular charge-transfer (ICT) character has been observed in many oligomers[30−48] and polymers,[10−12,36,49−66] that are composed of multiple building blocks with different electron affinities in each repeating unit, giving rise to ICT character across the conjugated backbone. Such CT bands are red-shifted from the $\pi \rightarrow \pi^*$ transition band of the corresponding homooligomers or homopolymers, as demonstrated in a series of thiophene oligomers with a single, high electron affinity thienothiophene block inserted in the middle,[67] and by a series CTPs with different ratios of the donor and acceptor blocks.[68]

In the **PTBF** polymers, the electron affinity of **TT** is higher than that of **BDT**,[7] so that the electron density is drawn from **BDT** to **TT**. Because an electron-withdrawing fluorine is attached to **TT** or **a** in the single **-d-a-** motif, the electron density further shifts to the **TT** direction, resulting in a higher local electron density gradient as well as a larger $\Delta\mu_{eg}$. In contrast, when **BDT** or **d** in the **-d-a-** motif is fluorinated as in **PTBF2**, the electron density is drawn in the opposite direction, partially canceling the electron density polarization when no fluorine is attached. Compared with **PTBF0**, **PTBF1** (with one fluorine attached to **TT** and the largest $\Delta\mu_{eg}$) drastically enhanced the CS state population but yielded no obvious effects on the EX, CT, and CS state decay dynamics. Compared with **PTBF1**, the fluorination of **BDT** in **PTBF2** and **PTBF3** prolongs the CT state lifetimes and accelerates the CS state decay. These results suggest that a more polarized exciton is more likely to produce a better separated hole and electron, which experiences less Coulombic attraction and, hence, is more likely to become free charge carriers. In contrast, a less polarized exciton could yield a more tightly bound hole−electron pair in the CT state and is more likely to recombine geminately. These observations are modeled with the $\Delta\mu_{eg}$ parameters (Table S3 in the Supporting Information)[7] of the single repeating units in these polymers, which reflect the local electron density displacement upon excitation, although they currently remain as empirical parameters. Comprehensive studies correlating $\Delta\mu_{eg}$ with the exciton state structure in long polymer chains are currently in progress. While this correlation is known now for a variety of CTPs,[15] understanding the underlying relationship is crucial to gain insight for optimization of next-generation OPV materials.

The potential energy surface for a hole and electron separated by distance r can be modeled by Onsager theory under thermal equilibrium,[13,69] where a parameter for the capture radius r_c is defined as the separation distance between a hole and an electron at which the electrostatic energy ($e^2/(4\pi\varepsilon_r\varepsilon_0 r_c)$) based on the Coulomb's Law equals the thermal energy k_BT and is given by $r_c = (e^2/(4\pi\varepsilon_r\varepsilon_0 k_BT))$, where e is the elementary charge, ε_r is the dielectric constant of the surrounding matrix, ε_0 is the permittivity of free space, k_B is Boltzmann's constant, and T is temperature. For r larger than r_c, k_BT surpasses the Coulombic attraction. Because the EX dissociation in the PTBF polymers results in a wide distribution of the hole−electron distances, the thermal energy gained from the ultrafast vibrational relaxation due to an excess of the excitation energy could only assist the CS state population with r slightly less than r_c to overcome the Columbic interactions. The polymers with a higher EX polarity can result in on average longer hole−electron distances than those with lower EX polarity as previously described, and hence the extra thermal energy could assist more hole−electron pairs to free carriers in the former than the latter.

In summary, exciton dissociation dynamics of the **PTBF** series in BHJ films were obtained via ultrafast NIR TA measurements, in which the dynamics and relative populations of CS and CT states are recorded to address the effect of local structure in **PTBF** polymers. The cation peak shifts were captured and shown as a good indicator following the hole−electron distance after the initial charge separation. We propose that the intramolecular CT character in these polymers can influence the initial energy of the hole−electron pair and the long-lasting detrapping process through the intrinsic polarity of the excitons. When the exciton has a higher polarity due to the push−pull actions between the neighboring building blocks of the CTPs, its dissociation results in CS hole−electron pairs with larger separation distances, enabling a higher probability to populate the CS state near or above the k_BT threshold as well as further evolve into free carriers. These results highlight the importance and correlation of local CT character in CTPs to their corresponding OPV device performance.

METHODS

Sample Preparation. PTBF polymers were synthesized as previously described[11,12] and spin-coated from 10 mg/mL chlorobenzene solutions onto glass substrates at 1000 rpm for 1 min. For BHJ films, **$PC_{71}BM$** was included in this PTBF solution in a 1:1.5 **PTBF/$PC_{71}BM$** molar ratio. 3% diiodooctane (DIO) additive was included because it is known to break up PCBM aggregates in solution.[70]

Near-Infrared Optical Transient Absorption. NIR optical TA spectroscopy was conducted on BHJ **PTBF/$PC_{71}BM$**/DIO polymer films. The laser setup has been described previously.[7] The experiments were conducted at room temperature using a motorized stage that rastered along the film at a speed of 1 mm/s to eliminate photodegradation effects. In previous

dx.doi.org/10.1021/jz5005957 | J. Phys. Chem. Lett. 2014, 5, 1856−1863

studies comparing the TA difference for **PTBF** films studied in air and in encapsulated films with active layers that were never exposed to ambient air, the difference in exciton dynamics on the time scale of the relevant dynamics discussed here, 100 fs to hundreds of picoseconds, is completely negligible.[6] Using this setup, 2-D NIR TA data sets were obtained along wavelength and time axes.

■ ASSOCIATED CONTENT

Supporting Information

Details of the fitting process and fit results. This material is available free of charge via the Internet at http://pubs.acs.org.

■ AUTHOR INFORMATION

Corresponding Authors

*E-mail: lchen@anl.gov or l-chen@northwestern.edu (L.C.).
*E-mail: lupingyu@uchicago.edu (L.Y.).

Present Addresses

[⊗]J.M.S.: Department of Chemistry, Lafayette College, 232 Hugel Science Center, Easton, PA 18042-1768, United States. [⊥]H.J.S.: Photoelectronic Hybrids Research Center, Korea Institute of Science and Technology (KIST), Hwarang-ro 14-gil 5, Seongbuk-gu, Seoul 136-791, Republic of Korea.

Notes

The authors declare no competing financial interest.

■ ACKNOWLEDGMENTS

This research was supported through the ANSER Center, an Energy Frontier Research Center funded by the U.S. Department of Energy, Office of Science, Office of Basic Energy Sciences, under Award Number DE-SC0001059 and the lab equipment was supported through the Division of Chemical Sciences, Office of Basic Energy Sciences, the U.S. Department of Energy under contract DE-AC02-06CH11357 (for L.X.C.). The gift from Intel Corp. to L.X.C. and L.P.Y. is greatly appreciated for a part of research related to film fabrication. We also thank Drs. D. J. Gosztola and G. P. Wiederrecht for their support in the Center for Nanoscale Materials at Argonne National Laboratory. Use of the facilities at the Center for Nanoscale Materials was supported by the U.S. Department of Energy, Office of Science, Office of Basic Energy Sciences, under Contract No. DE-AC02-06CH11357. L.P.Y. acknowledges support by U. S. National Science Foundation grants, Air Force Office of Scientific Research and NSF MRSEC program at the University of Chicago.

■ REFERENCES

(1) Lewis, N. S.; Nocera, D. G. Powering the Planet: Chemical Challenges in Solar Energy Utilization. *Proc. Nat. Acad. Sci.* **2006**, *103* (43), 8.

(2) Branker, K.; Pathak, M. J. M.; Pearce, J. M. a Review of Solar Photovoltaic Levelized Cost of Electricity. *Renewable Sustainable Energy Rev.* **2011**, *15* (9), 4470−4482.

(3) Blankenburg, L.; Schultheis, K.; Schache, H.; Sensfuss, S.; Schrödner, M. Reel-to-Reel Wet Coating As an Efficient up-Scaling Technique for the Production of Bulk-Heterojunction Polymer Solar Cells. *Sol. Energy Mater. Sol. Cells* **2009**, *93*, 476−483.

(4) Barnett, A.; Kirkpatrick, D.; Honsberg, C.; Moore, D.; Wanlass, M.; Emery, K.; Schwartz, R.; Carlson, D.; Bowden, S.; Aiken, D.; Gray, A.; Kurtz, S.; Kazmerski, L.; Steiner, M.; Gray, J.; Davenport, T.; Buelow, R.; Takacs, L.; Shatz, N.; Bortz, J.; Jani, O.; Goossen, K.; Kiamilev, F.; Doolittle, A.; Ferguson, I.; Unger, B.; Schmidt, G.; Christensen, E.; Salzman, D. Very High Efficiency Solar Cell Modules. *Prog. Photovoltaics* **2009**, *17* (1), 75−83.

(5) Polyera Achieves Certified 9.1% Efficiency for Polymer Photovoltaic Devices. http://www.osa-direct.com/osad-news/polyera-achieves-certified-91-efficiency-for-polymer-photovoltaic-devices.html.

(6) Szarko, J. M.; Rolczynski, B. S.; Lou, S. J.; Xu, T.; Strzalka, J.; Marks, T. J.; Yu, L.; Chen, L. X. Photovoltaic Function and Exciton/Charge Transfer Dynamics in a Highly Efficient Semiconducting Copolymer. *Adv. Funct. Mater.* **2014**, *24* (1), 10−26.

(7) Rolczynski, B. S.; Szarko, J. M.; Son, H.-J.; Liang, Y.; Yu, L.; Chen, L. X. Ultrafast Intramolecular Exciton Splitting Dynamics in Isolated Low-Band-Gap Polymers and Their Implications in Photovoltaic Materials Design. *J. Am. Chem. Soc.* **2012**, *134* (9), 4142−4152.

(8) Bakulin, A. A.; Rao, A.; Pavelyev, V. G.; van Loosdrecht, P. H. M.; Pshenichnikov, M. S.; Niedzialek, D.; Cornil, J.; Beljonne, D.; Friend, R. H. The Role of Driving Energy and Delocalized States for Charge Separation in Organic Semiconductors. *Science* **2012**, *335* (6074), 1340−1344.

(9) Ohkita, H.; Cook, S.; Astuti, Y.; Duffy, W.; Tierney, S.; Zhang, W.; Heeney, M.; Mcculloch, I.; Nelson, J.; Bradley, D. D. C.; Durrant, J. R. Charge Carrier Formation in Polythiophene/Fullerene Blend Films Studied by Transient Absorption Spectroscopy. *J. Am. Chem. Soc.* **2008**, *130* (10), 3030−3042.

(10) Liang, Y.; Xu, Z.; Xia, J.; Tsai, S.-T.; Wu, Y.; Li, G.; Ray, C.; Yu, L. For the Bright Future-Bulk Heterojunction Polymer Solar Cells with Power Conversion Efficiency of 7.4%. *Adv. Mater.* **2010**, *22* (20), E135−E138.

(11) Liang, Y.; Feng, D.; Wu, Y.; Tsai, S.-T.; Li, G.; Ray, C.; Yu, L. Highly Efficient Solar Cell Polymers Developed via Fine-Tuning of Structural and Electronic Properties. *J. Am. Chem. Soc.* **2009**, *131*, 7792−7799.

(12) Son, H. J.; Wang, W.; Xu, T.; Liang, Y.; Wu, Y.; Li, G.; Yu, L. Synthesis of Fluorinated Polythienothiophene-co-benzodithiophenes and Effect of Fluorination on the Photovoltaic Properties. *J. Am. Chem. Soc.* **2011**, *133*, 1885−1894.

(13) Clarke, T. M.; Durrant, J. R. Charge Photogeneration in Organic Solar Cells. *Chem. Rev.* **2010**, 32.

(14) Banerji, N. Sub-Picosecond Delocalization in the Excited State of Conjugated Homopolymers and Donor−acceptor Copolymers. *J. Mater. Chem. C* **2013**, *1* (18), 3052.

(15) Carsten, B.; Szarko, J. M.; Lu, L.; Son, H.-J.; He, F.; Botros, Y. Y.; Chen, L. X.; Yu, L. Mediating Solar Cell Performance by Controlling the Internal Dipole Change in Organic Photovoltaic Polymers. *Macromolecules* **2012**, *45* (16), 6390−6395.

(16) Carsten, B.; Szarko, J. M.; Son, H.-J.; Wang, W.; Lu, L.; He, F.; Rolczynski, B. S.; Lou, S. J.; Chen, L. X.; Yu, L. Examining the Effect of the Dipole Moment on Charge Separation in Donor−Acceptor Polymers for Organic Photovoltaic Applications. *J. Am. Chem. Soc.* **2011**, *133* (50), 20468−20475.

(17) Beenken, W. J. D.; Pullerits, T. Spectroscopic Units in Conjugated Polymers: A Quantum Chemically Founded Concept? *J. Phys. Chem. B* **2004**, *108*, 6164−6169.

(18) Jackson, N. E.; Savoie, B. M.; Kohlstedt, K. L.; Olvera de la Cruz, M.; Schatz, G. C.; Chen, L. X.; Ratner, M. A. Controlling Conformations of Conjugated Polymers and Small Molecules: The Role of Nonbonding Interactions. *J. Am. Chem. Soc.* **2013**, *135* (28), 10475−10483.

(19) Guo, J.; Ohkita, H.; Benten, H.; Ito, S. Near-IR Femtosecond Transient Absorption Spectroscopy of Ultrafast Polaron and Triplet Exciton Formation in Polythiophene Films with Different Regioregularities. *J. Am. Chem. Soc.* **2009**, *131* (12), 16869−16880.

(20) Carmichael, I.; Hug, G. Triplet-Triplet Absorption-Spectra of Organic-Molecules in Condensed Phases. *J. Phys. Chem. Ref. Data* **1986**, *15* (1), 1−250.

(21) Seki, H. Effect of Salts on the Quantum Yield and the Decay of Lons Produced by Photoinduced Electron Transfer from Zinc Tetraphenylporphyrin to 1,4-Benzoquinone in 4-Methylpentan-2-one. *Faraday Trans.* **1992**, *88* (1), 35.

(22) Langan, J. R.; Salmon, G. A. Pulse Radiolysis of Solutions of Trans-Stilbene. Radical-Anions and Ion-Pairs in Tetrahydrofuran. *J. Chem. Soc., Faraday Trans. 1* **1982**, *78* (12), 3645.
(23) Yamamoto, Y.; Aoyama, T.; Hayashi, K. Pulse Radiolysis Study of Salt Effects on Reactions of Aromatic Radical Cations with Cl-. Part 2. Spectral Shifts and Decay Kinetics of Diphenylpolyene Radical Cations in the Presence of Tetrabutylammonium Hexafluorophosphate. *J. Chem. Soc., Faraday Trans. 1* **1988**, *84* (6), 2209.
(24) Yamamoto, Y.; Nishida, S.; Ma, X.-H.; Hayashi, K. Pulse Radiolysis of trans-Stilbene in Tetrahydrofuran. Spectral Shift and Decay Kinetics of the Radical Anions in the Presence of Quaternary Ammonium Salts. *J. Phys. Chem.* **1986**, *90* (9), 1921−1924.
(25) Gersdorf, J.; Mattay, J.; Gorner, H. Photoreactions of Biacetyl, Benzophenone, and Benzil with Electron-Rich Alkenes. *J. Am. Chem. Soc.* **1987**, *109* (1203), 1203−1209.
(26) Garcia, A.; Brzezinski, J. Z.; Nguyen, T.-Q. Cationic Conjugated Polyelectrolyte Electron Injection Layers: Effect of Halide Counterions. *J. Phys. Chem. C* **2009**, *113* (7), 2950−2954.
(27) Gregg, B. A. Entropy of Charge Separation in Organic Photovoltaic Cells: The Benefit of Higher Dimensionality. *J. Phys. Chem. Lett.* **2011**, *2* (24), 3013−3015.
(28) Hammond, M. R.; Kline, R. J.; Herzing, A. A.; Richter, L. J.; Germack, D. S.; Ro, H.-W.; Soles, C. L.; Fischer, D. A.; Xu, T.; Yu, L.; Toney, M. F.; DeLongchamp, D. M. Molecular Order in High-Efficiency Polymer/Fullerene Bulk Heterojunction Solar Cells. *ACS Nano* **2011**, *5* (10), 8248−8257.
(29) Barbour, L. W.; Hegadorn, M.; Asbury, J. B. Watching Electrons Move in Real Time: Ultrafast Infrared Spectroscopy of a Polymer Blend Photovoltaic Material. *J. Am. Chem. Soc.* **2007**, *129* (51), 15884−15894.
(30) Tian, H.; Yang, X.; Pan, J.; Chen, R.; Liu, M.; Zhang, Q.; Hagfeldt, A.; Sun, L. A Triphenylamine Dye Model for the Study of Intramolecular Energy Transfer and Charge Transfer in Dye-Sensitized Solar Cells. *Adv. Funct. Mater.* **2008**, *18* (21), 3461−3468.
(31) Lincker, F.; Delbosc, N.; Bailly, S.; De Bettignies, R.; Billon, M.; Pron, A.; Demadrille, R. Fluorenone-Based Molecules for Bulk-Heterojunction Solar Cells: Synthesis, Characterization, and Photovoltaic Properties. *Adv. Funct. Mater.* **2008**, *18* (21), 3444−3453.
(32) Cho, N.; Kim, J.; Song, K.; Lee, J. K.; Ko, J. Synthesis and Characterization of Push-Pull Organic Semiconductors with Various Acceptors for Solution-Processed Small Molecule Organic Solar Cells. *Tetrahedron* **2012**, *68* (21), 4029−4036.
(33) Yassar, A.; Videlot, C.; Jaafari, A. Synthesis and Photovoltaic Properties of Mono-Substituted Quaterthiophenes Bearing Strong Electron-Withdrawing Group. *Sol. Energy Mater. Sol. Cells* **2006**, *90* (7−8), 916−922.
(34) SaKong, C.; Kim, S.-H.; Yuk, S. B.; Kim, J.-Y.; Park, S.-W.; Ko, M.-J.; Kim, J. P. Synthesis of Novel Quinacridone Dyes and Their Photovoltaic Performances in Organic Dye-Sensitized Solar Cells. *Bull. Korean Chem. Soc.* **2011**, *32* (8), 2553−2559.
(35) Li, Z.; Dong, Q.; Xu, B.; Li, H.; Wen, S.; Pei, J.; Yao, S.; Lu, H.; Li, P.; Tian, W. New Amorphous Small Molecules—synthesis, Characterization and Their Application in Bulk Heterojunction Solar Cells. *Sol. Energy Mater. Sol. Cells* **2011**, *95* (8), 2272−2280.
(36) Li, Y.; Li, Z.; Wang, C.; Li, H.; Lu, H.; Xu, B.; Tian, W. Novel Low-Bandgap Oligothiophene-Based Donor-Acceptor Alternating Conjugated Copolymers: Synthesis, Properties, And Photovoltaic Applications. *J. Polym. Sci., Part A: Polym. Chem.* **2010**, *48* (13), 2765−2776.
(37) Li, W.; Wu, Y.; Zhang, Q.; Tian, H.; Zhu, W. D-A-π-A Featured Sensitizers Bearing Phthalimide and Benzotriazole as Auxiliary Acceptor: Effect on Absorption and Charge Recombination Dynamics in Dye-Sensitized Solar Cells. *ACS Appl. Mater. Interfaces* **2012**, *4* (3), 1822−1830.
(38) Li, Z.; Dong, Q.; Li, Y.; Xu, B.; Deng, M.; Pei, J.; Zhang, J.; Chen, F.; Wen, S.; Gao, Y.; Tian, W. Design and Synthesis of Solution Processable Small Molecules Towards High Photovoltaic Performance. *J. Mater. Chem.* **2011**, *21* (7), 2159.
(39) Pai, C.-L.; Liu, C.-L.; Chen, W.-C.; Jenekhe, S. A. Electronic Structure and Properties of Alternating Donor−Acceptor Conjugated Copolymers: 3,4-Ethylenedioxythiophene (EDOT) Copolymers and Model Compounds. *Polymer* **2006**, *47* (2), 699−708.
(40) He, Q.; He, C.; Sun, Y.; Wu, H.; Li, Y.; Bai, F. Amorphous Molecular Material Containing Bisthiophenyl-Benzothiadiazole and Triphenylamine with Bipolar and Low-Bandgap Characteristics for Solar Cells. *Thin Solid Films* **2008**, *516* (18), 5935−5940.
(41) Song, S.; Han, H.; Kim, Y.; Lee, B. H.; Park, S. H.; Jin, Y.; Kim, I.; Lee, K.; Suh, H. Dimethyl-2H-benzimidazole Based Small Molecules As Donor Materials for Organic Photovoltaics. *Sol. Energy Mater. Sol. Cells* **2011**, *95* (7), 1838−1845.
(42) Isla, H.; Grimm, B.; Pérez, E. M.; Rosario Torres, M.; Ángeles Herranz, M.; Viruela, R.; Aragó, J.; Orti, E.; M Guldi, D.; Martín, N. Bowl-Shape Electron Donors with Absorptions in the Visible Range of the Solar Spectrum and Their Supramolecular Assemblies with C60. *Chem. Sci.* **2012**, *3* (2), 498.
(43) Kim, J.; Cho, N.; Ko, H. M.; Kim, C.; Lee, J. K.; Ko, J. Push-Pull Organic Semiconductors Comprising of Bis-Dimethylfluorenyl Amino Benzo[B]Thiophene Donor and Various Acceptors for Solution Processed Small Molecule Organic Solar Cells. *Sol. Energy Mater. Sol. Cells* **2012**, *102* (C), 159−166.
(44) Cheng, Y.-J.; Chen, C.-H.; Ho, Y.-J.; Chang, S.-W.; Witek, H. A.; Hsu, C.-S. Thieno[3,2-b]pyrrolo Donor Fused with Benzothiadiazolo, Benzoselenadiazolo and Quinoxalino Acceptors: Synthesis, Characterization, and Molecular Properties. *Org. Lett.* **2011**, *13* (20), 5484−5487.
(45) Zeng, S.; Yin, L.; Jiang, X.; Li, Y.; Li, K. D-A-D Low Band Gap Molecule Containing Triphenylamine and Benzoxadiazole/Benzothiadiazole Units: Synthesis and Photophysical Properties. *Dyes Pigm.* **2012**, *95* (2), 229−235.
(46) Li, Z.; Pei, J.; Li, Y.; Xu, B.; Deng, M.; Liu, Z.; Li, H.; Lu, H.; Li, Q.; Tian, W. Synthesis and Photovoltaic Properties of Solution Processable Small Molecules Containing 2-Pyran-4-ylidenemalononitrile and Oligothiophene Moieties. *J. Phys. Chem. C* **2010**, *114* (42), 18270−18278.
(47) Gong, Y.; Guo, X.; Wang, S.; Su, H.; Xia, A.; He, Q.; Bai, F. Photophysical Properties of Photoactive Molecules with Conjugated Push−Pull Structures. *J. Phys. Chem. A* **2007**, *111* (26), 5806−5812.
(48) Liang, Y.; Feng, D.; Guo, J.; Szarko, J. M.; Ray, C.; Chen, L. X.; Yu, L. Regioregular Oligomer and Polymer Containing Thieno[3,4-b]thiophene Moiety for Efficient Organic Solar Cells. *Macromolecules* **2009**, *42* (4), 8.
(49) Skabara, P. J.; Berridge, R.; Serebryakov, I. M.; Kanibolotsky, A. L.; Kanibolotskaya, L.; Gordeyev, S.; Perepichka, I. F.; Sariciftci, N. S.; Winder, C. Fluorene Functionalised Sexithiophenes? Utilising Intramolecular Charge Transfer to Extend the Photocurrent Spectrum in Organic Solar Cells. *J. Mater. Chem.* **2007**, *17* (11), 1055.
(50) Lee, J. Y.; Choi, M. H.; Heo, S. W.; Moon, D. K. Synthesis of random copolymers based on 3-hexylthiophene and quinoxaline derivative: Influence between the intramolecular charge transfer (ICT) effect and Ï€-conjugation length for their photovoltaic properties. *Synth. Met.* **2011**, *161* (1−2), 1−6.
(51) Choi, Y.-S.; Lee, W.-H.; Kim, J.-R.; Lee, S.-K.; Shin, W. S.; Moon, S.-J.; Park, J.-W.; Kang, I.-N. Synthesis and Characterization of Quinoxaline-Based Thiophene Copolymers as Photoactive Layers in Organic Photovoltaic Cells. *Bull. Korean Chem. Soc.* **2011**, *32* (2), 417−423.
(52) Jung, I. H.; Kim, S. H.; Jeong, E.; Yang, R.; Lee, K.; Woo, H. Y.; Shim, H.-K. Synthesis and Characterization of Fluorene and Cyclopentadithiophene-Based Copolymers Exhibiting Broad Absorption for Photovoltaic Devices. *J. Polym. Sci., Part A: Polym. Chem.* **2011**, *49* (5), 1248−1255.
(53) Kim, Y.-G.; Thompson, B. C.; Ananthakrishnan, N.; Padmanaban, G.; Ramakrishnan, S.; Reynolds, J. R. Variable Band Gap Conjugated Polymers for Optoelectronic and Redox Applications. *J. Mater. Res.* **2005**, *20* (12), 3188−3198.
(54) Cheng, Y.-J.; Hung, L.-C.; Cao, F.-Y.; Kao, W.-S.; Chang, C.-Y.; Hsu, C.-S. Alternating Copolymers Incorporating Cyclopenta[2,1-

b:3,4-b′]dithiophene Unit and Organic Dyes for Photovoltaic Applications. *J. Polym. Sci., Part A: Polym. Chem.* **2011**, *49* (8), 1791−1801.
(55) Li, Y.; Li, H.; Xu, B.; Li, Z.; Chen, F.; Feng, D.; Zhang, J.; Tian, W. Molecular Structure-Property Engineering for Photovoltaic Applications: Fluorene-Acceptor Alternating Conjugated Copolymers with Varied Bridged Moieties. *Polymer* **2010**, *51* (8), 1786−1795.
(56) Jung, I. H.; Yu, J.; Jeong, E.; Kim, J.; Kwon, S.; Kong, H.; Lee, K.; Woo, H. Y.; Shim, H.-K. Synthesis and Photovoltaic Properties of Cyclopentadithiophene-Based Low-Bandgap Copolymers That Contain Electron-Withdrawing Thiazole Derivatives. *Chem.—Eur. J.* **2010**, *16* (12), 3743−3752.
(57) Guo, X.; Xin, H.; Kim, F. S.; Liyanage, A. D. T.; Jenekhe, S. A.; Watson, M. D. Thieno[3,4- c]pyrrole-4,6-dione-Based Donor−Acceptor Conjugated Polymers for Solar Cells. *Macromolecules* **2011**, *44* (2), 269−277.
(58) Beaujuge, P. M.; Amb, C. M.; Reynolds, J. R. Spectral Engineering in π-Conjugated Polymers with Intramolecular Donor−Acceptor Interactions. *Acc. Chem. Res.* **2010**, *43* (11), 1396−1407.
(59) Ranjith, K.; Swathi, S. K.; Kumar, P.; Ramamurthy, P. C. Dithienylcyclopentadienone Derivative-co-benzothiadiazole An Alternating Copolymer for Organic Photovoltaics. *Sol. Energy Mater. Sol. Cells* **2012**, *98* (C), 448−454.
(60) Li, Y.; Xue, L.; Li, H.; Li, Z.; Xu, B.; Wen, S.; Tian, W. Energy Level and Molecular Structure Engineering of Conjugated Donor−Acceptor Copolymers for Photovoltaic Applications. *Macromolecules* **2009**, *42* (13), 4491−4499.
(61) Braunecker, W. A.; Owczarczyk, Z. R.; Garcia, A.; Kopidakis, N.; Larsen, R. E.; Hammond, S. R.; Ginley, D. S.; Olson, D. C. Benzodithiophene and Imide-Based Copolymers for Photovoltaic Applications. *Chem. Mater.* **2012**, *24* (7), 1346−1356.
(62) Liu, C.-L.; Tsai, J.-H.; Lee, W.-Y.; Chen, W.-C.; Jenekhe, S. A. New Didecyloxyphenylene−Acceptor Alternating Conjugated Copolymers: Synthesis, Properties, and Optoelectronic Device Applications. *Macromolecules* **2008**, *41* (19), 6952−6959.
(63) Peng, Q.; Liu, X.; Qin, Y.; Zhou, D.; Xu, J. Thieno[3,4-b]pyrazine-Based Low Bandgap Photovoltaic Copolymers: Turning the Properties by Different Aza-Heteroaromatic Donors. *J. Polym. Sci., Part A: Polym. Chem.* **2011**, *49* (20), 4458−4467.
(64) Liang, Y.; Wu, Y.; Feng, D.; Tsai, S.-T.; Son, H.-J.; Li, G.; Yu, L. Development of New Semiconducting Polymers for High Performance Solar Cells. *J. Am. Chem. Soc.* **2009**, *131*, 3.
(65) Liang, Y.; Yu, L. A New Class of Semiconducting Polymers for Bulk Heterojunction Solar Cells with Exceptionally High Performance. *Acc. Chem. Res.* **2010**, *43* (9), 1227−1236.
(66) Mühlbacher, D.; Scharber, M.; Morana, M.; Zhu, Z.; Waller, D.; Gaudiana, R.; Brabec, C. High Photovoltaic Performance of a Low-Bandgap Polymer. *Adv. Mater.* **2006**, *18* (21), 2884−2889.
(67) Szarko, J. M.; Rolczynski, B. S.; Guo, J.; Liang, Y.; He, F.; Mara, M. W.; Yu, L.; Chen, L. X. Electronic Processes in Conjugated Diblock Oligomers Mimicking Low Band-Gap Polymers: Experimental and Theoretical Spectral Analysis. *J. Phys. Chem. B* **2010**, *114*, 14505−14513.
(68) Liang, Y.; Xiao, S.; Feng, D.; Yu, L. Control in Energy Levels of Conjugated Polymers for Photovoltaic Application. *J. Phys. Chem. C* **2008**, *112*, 7866−7871.
(69) Onsager, L. Initial Recombination of Ions. *Phys. Rev.* **1938**, *54*, 554−557.
(70) Lou, S. J.; Szarko, J. M.; Xu, T.; Yu, L.; Marks, T. J.; Chen, L. X. Effects of Additives on the Morphology of Solution Phase Aggregates Formed by Active Layer Components of High-Efficiency Organic Solar Cells. *J. Am. Chem. Soc.* **2011**, *133* (51), 20661−20663.